

# Hybrid Titania Microspheres of Novel Superstructures Templated by Block Copolymers

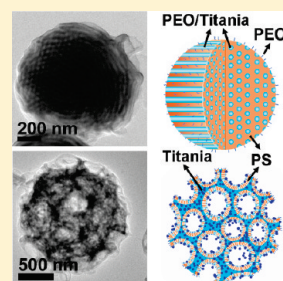
Yu Zhang, Happy Tan, Hui Li, Yan-Qiong Liu, Fransiska C. Kartawidjaja, Zheng-Chun Yang, and John Wang\*

Department of Materials Science and Engineering, National University of Singapore, Singapore, 117576

 Supporting Information

**ABSTRACT:** Two new titania-based nanostructures—namely, hexagonally packed titania hoops (HTHs) and modified large compound vesicles (LCVs)—were created in polystyrene-*b*-poly(ethylene oxide) (PS-*b*-PEO)/titania microspheres by coupling self-assembly of the asymmetric amphiphilic block copolymers in selective solvents with the sol–gel process of titania. The formation of these nanostructures was induced by solvent evaporation, where the evaporation rate difference between tetrahydrofuran and water, under certain ambient humidity, strongly affects the nanostructure resulted by changing the force balance, principally involving the stretching of the PS blocks, the surface tension between the PS and the surrounding solvents, and the repulsive interactions among the PEO chains. When the relative humidity of the evaporation process was controlled at 67%, a modified LCVs structure was formed involving a morphology evolution initially from lamellae to large polydisperse vesicles and then to modified LCVs. As the relative humidity decreased from 67% to 30%, the modified LCVs transferred to the HTHs structure, which is ascribed to the reduction of the effective volume fraction of the PEO blocks associated with the decrease in humidity. Stable anatase microspheres of either HTHs or modified LCVs morphology were obtained upon calcination at 500 °C.

**KEYWORDS:** hexagonally packed titania hoops, large compound vesicles, self-assembly, sol–gel, titania



## INTRODUCTION

Synthesis of nanoscale titania materials is one of the most active research areas, because of the widespread use of titania in photocatalysis, photovoltaics, lithium-ion batteries, and sensing devices. A remarkably diverse and growing range of titania nanostructures has been synthesized, including nanoparticles, nanorods, nanowires, nanotubes, and mesoporous titania of hexagonal, cubic, or lamellar pore organization.<sup>1–4</sup> In these titania nanostructures, there is a strong dependence of the functional performance on the morphology and length scales.

Among various synthesis approaches, self-assembly of block copolymers in selective solvents has proven its great versatility in templating inorganic nanomaterials with exquisite morphologies and novel functional properties.<sup>5</sup> The concept was thoroughly discussed in the work of Sanchez et al.,<sup>2</sup> Smarsly et al.,<sup>2d,3</sup> and Ozin et al.,<sup>4</sup> who reported the formation of mesostructured titania composed of periodically arranged nanosized pores. The block copolymers that were applied exhibited a longer solvophilic block forming the corona than the solvophobic block forming the core, giving rise to star micelles.<sup>2–4</sup>

In contrast to the star micelles, the so-called “crew-cut micelles” represent a relatively new type of micelles that has been receiving growing attention since Eisenberg and co-workers studied the self-assembly behavior of asymmetric amphiphilic block copolymers of polystyrene-*b*-poly(acrylic acid) (PS-*b*-PAA) in solution in 1995.<sup>6</sup> They are characterized by a bulky core formed by the long solvophobic blocks and a relatively small corona formed by the short solvophilic blocks. Crew-cut micelles

possess a rich variety of morphologies, including not only the simple morphologies (such as spheres, rods, and vesicles), but also some complex superstructures (such as hollow concentric vesicles, onions, large compound vesicles (LCVs), and hexagonally packed hollow hoops (HHHs)).<sup>7</sup> They therefore provide a versatile platform to template metallic, semiconductive, and other inorganic nanostructures. For example, inorganic nanoparticles (e.g., PbS, LaOF, TiO<sub>2</sub>, Fe<sub>2</sub>O<sub>3</sub>, and core–shell CdSe/ZnS) have been incorporated in crew-cut spheres, rods, and vesicles of block copolymers.<sup>8,9</sup> Macroporous films,<sup>10</sup> nanorods,<sup>1</sup> and nanovesicles of silica or titania have been templated by crew-cut spheres, rods, and vesicles, respectively.<sup>11–17</sup> However, inorganic replication of complex crew-cut superstructures is less common. Two pioneer works have been carried out for the development of poly(ethylene oxide)-*b*-poly(3-(trimethoxysilyl) propyl methacrylate) (PEO-*b*-PTMSPMA)/polysilsesquioxane LCVs and PS-*b*-PEO/silica concentric vesicles, respectively.<sup>18,19</sup>

In this paper, by coupling the self-assembly of block copolymers of PS-*b*-PEO in selective solvents with the sol–gel chemistry of titanium precursors, we report a successful synthesis of PS-*b*-PEO/titania hybrid microspheres with unprecedented hexagonally packed titania hoops (HTHs) and modified LCVs morphologies. Their counterparts in the crew-cut family of block copolymers are HHHs and LCVs, respectively. HHHs refers to

**Received:** November 11, 2010

**Revised:** April 18, 2011

**Published:** May 11, 2011

amphiphilic block copolymer aggregates with an internal structure of hollow hoops hexagonally packed in the solvophobic-block-formed matrix, and both the external surface of the aggregates and the internal surface of the hollow hoops are lined with solvophilic chains. It is the only ordered morphology in the crew-cut family, and it has attracted a great deal of interest since it was first indexed by Zhang and co-workers.<sup>20–22</sup> However, mineralization of the complex HHHs morphology has never been achieved. LCVs are generally assemblies of many vesicles, composed of vesicular compartments separated by a copolymer matrix. In the modified LCVs hybrids synthesized in the present study, bowl-shaped vesicles instead of simple vesicles become the constituent units. This multicompartment structure not only increases the surface area but also allows encapsulation of various functional objects such as drugs and inorganic nanoparticles. Titanium species are attached to the hydrophilic PEO chains localized at both the interior and exterior surfaces of the constituent vesicles. It is different from the PEO-*b*-PTMSPMA/polysilsesquioxane LCVs previously reported,<sup>18</sup> where Si-oxo groups were incorporated in the hydrophobic vesicle walls. The continuous three-dimensional inorganic framework produced by cross-linking of Ti-oxo is essential for enhanced mechanical and physical properties.

In addition, we have investigated the ambient humidity effect on morphology during the evaporation process. The formation mechanisms of both the HTHs and modified LCVs organic–inorganic hybrid structures are proposed, based on the previous studies on the crew-cut HHHs and LCVs morphologies for diblock copolymers,<sup>20,21</sup> and the intermediate structures observed during the morphology evolution in this study.

## EXPERIMENTAL SECTION

An asymmetric diblock copolymer of PS-*b*-PEO ( $M_n = 18000 \text{ g mol}^{-1}$  for PS and  $7500 \text{ g mol}^{-1}$  for PEO, with a polydispersity of 1.05 and PS content of 70 wt %) was purchased from Polymer Source, Inc. Titanium tetraisopropoxide (TTIP, 97%) and tetrahydrofuran (THF) were purchased from Aldrich. HCl (37%) was purchased from Merck.

Typically, PS-*b*-PEO was first dissolved in THF and stirred for 1 h. A colorless clear solution was obtained thereafter. TTIP and 37% HCl were subsequently added dropwise into the solution. The molar ratios of these ingredients were controlled as follows: PS-*b*-PEO/THF/TTIP/HCl/H<sub>2</sub>O = 0.001:9:0.3:1.8:6.21 (H<sub>2</sub>O applied herein entirely arose from the 37% HCl solution). The system became orange-colored, translucent, and viscous, because the concentrated HCl is a precipitant for the PS blocks, which induces aggregation of the PS blocks in the solution. After stirring for another 3 h, the solution was transferred into a solvothermal bomb for annealing at 80 °C for 30 min. The resulted solution was still orange-colored and translucent. No precipitate was observed. The mixture was drop-cast on carbon coated Cu grids or glass substrates, followed by the solvent evaporation at ambient temperature and certain relative humidity (RH = 30% or 67%, respectively). The 30% RH condition was stringently controlled in a humidity control room, and the 67% RH condition was the normal laboratory humidity environment. The fluctuation level of RH is  $\pm 2\%$ . After drying, the as-deposited layer was calcined at 500 °C for 2 h ( $1 \text{ }^\circ\text{C min}^{-1}$  ramp) in air to remove the block copolymers and crystallize the titania framework.

As a comparison test, a solution was prepared following the same procedure, except that no TTIP was added.

Transmission electron microscopy (TEM) (JEOL, Model JEM 2010F, 200 kV) and field-emission scanning electron microscopy (SEM) (Philips XL 30 FEG-SEM) equipment was employed to investigate the morphology and texture of the copolymer/titania microspheres. Raman measurements

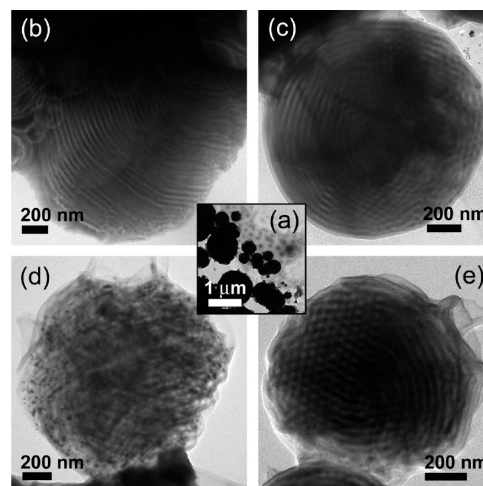


**Figure 1.** TEM images of PS-*b*-PEO/titania hybrid microspheres formed under 30% RH during the evaporation process.

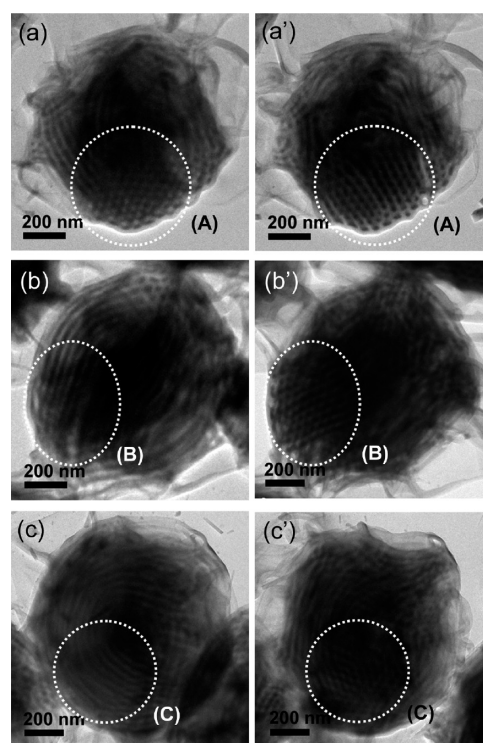


**Figure 2.** TEM images of PS-*b*-PEO/titania hybrid microspheres formed under 30% RH during the evaporation process: (a–c) images viewed at 0° tilt and (a'–c') corresponding images of the samples shown in panels a–c viewed at 18° tilt.

(using a Jobin–Yvon Model U1000 double monochromator) and XRD measurements (Bruker, Model AXS D8 Advance) were carried out for identification of the crystalline phase of the inorganic framework. XRD phase analyses were conducted in a  $\theta/2\theta$  Bragg–Brentano geometry, and  $2\theta$  varied over a range of  $20^\circ$ – $70^\circ$ . It was operated at 40 kV and 40 mA under Cu K $\alpha$  radiation ( $1.5406 \text{ \AA}$ ) with a step size of  $0.04^\circ$  and a time per step of 5 s. Fourier transform infrared (FTIR) spectrophotometer (Varian, Model 3100 Excalibur) and XPS (VG, Model ESCALAB 220I-XL, monochromatic Al K $\alpha$ , source (1486.6 eV)) were employed to identify the chemical composition of the copolymer/titania microspheres.



## RESULTS AND DISCUSSION

**Structure Characterization of PS-*b*-PEO/Titania Hybrid Microspheres.** Figures 1a–e show representative TEM images of the PS-*b*-PEO/titania hybrid aggregates prepared under 30% RH conditions during the evaporation process. The aggregates are near-spherical in shape, with a broad size distribution from hundreds of nanometers to several micrometers (Figure 1a). The aggregates, on first sight, seem to have several different internal configurations (Figures 1b–e). For example, the aggregates in Figures 1b and 1c display periodic structures composed of alternating dark and bright fringes or concentric circles, respectively. The aggregate in Figure 1d appears like a clew composed of bundles of dark threads crossing or intersecting with each other. A hexagonal array of bright spots is clearly seen near the left region of the aggregate shown in Figure 1e; the region on the right-hand side exhibits a pattern similar to that shown in Figures 1b and 1c.

Figure 2 shows three sets of TEM images of different aggregates taken at 0° tilt (Figures 2a–c) and 18° tilt (Figures 2a'–c'). Specifically, region (A) (Figures 2a and 2a') shows a pattern change from hexagonally packed bright spots (at 0° tilt) to dark spots (at 18° tilt), while the dimension remains the same; regions (B) (Figures 2b and 2b') and (C) (Figures 2c and 2c') show changes from a pattern of alternating dark and bright lines (at 0° tilt) to patterns of hexagonally packed dark spots or white spots (at 18° tilt), respectively. These structural features suggest that the different appearance of the internal structure of the aggregates could be a result of changes in the viewing angle of the aggregates, since the aggregates are randomly distributed on the TEM grid. Analogous phenomena have been observed in both PS-*b*-PAA and PS-*b*-PEO aggregates of an internal HHHs crew-cut morphology,<sup>20,22</sup> where the morphology was indexed using thorough imaging and simulation analyses. The similarity in the preparation procedure and the structure resulted suggests that the aggregates obtained in the present study possess an internal HHHs-like configuration. For block copolymer aggregates of an internal HHHs morphology, the hollow hoops with the internal surface lined with solvophilic chains are essentially filled with solvents in solution, and become empty after drying. For the PS-*b*-PEO/titania hybrid aggregates involved in the present study, the hollow hoops are filled with Ti-oxo species, which are linked through hydrogen bonds to the hydrophilic PEO chains decorating at the internal surface of the hoops. The dark regions as illustrated in the aforementioned TEM images are thus enriched with PEO/titania domains, which exhibit a higher electron density, compared to the bright region composed of PS domains, while both regions have an average width of ~20 nm.

Two issues must be clarified. First, varying appearances can be observed in TEM for different sections of an aggregate. It suggests that the aggregate may consist of several sections which are all of a HHHs pattern but with different hoop orientations. Second, the internal morphology of the hybrids, strictly speaking, should be identified as quasihexagonal, because a real HHHs structure requires a cylindrical or truncated cone-shaped external shape of the aggregates, which is unsatisfied by the near-spherical shape of the hybrid aggregates synthesized in this study. Nevertheless, considering the high ordering of the internal hexagonal pattern of the aggregates and their hybrid nature where solid titania hoops have replaced hollow hoops, the internal morphology of PS-*b*-PEO/titania hybrids is better identified as HTHs, a hybrid

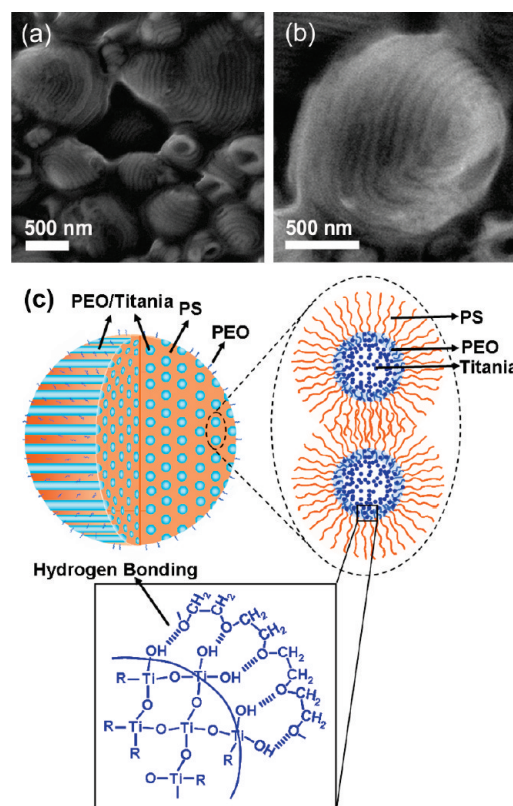


**Figure 3.** (a, b) SEM images of PS-*b*-PEO/titania hybrid microspheres formed under 30% RH during the evaporation process. (c) Schematic presentation of a PS-*b*-PEO/titania hybrid microsphere of an internal HTHs structure.

counterpart of the HHHs or quasihexagonal structure of block copolymer aggregates.

The SEM images shown in Figures 3a and 3b confirm the hoop structure at the aggregate surface, where the PEO/titania hoops (dark regions) are slightly concave to the PS matrix (light regions). It could well be due to an incomplete filling of the hollow hoop with PEO/titania species, or due to a lower surface tension of PS blocks than PEO blocks. It has been reported that a lower-surface-energy constituent of block copolymers preferentially locates itself at the free surface. Therefore, the PS fraction in PS-*b*-PEO diblock copolymers allows a degree of surface enrichment, because of the slightly lower surface energy of PS ( $0.036 \text{ N m}^{-1}$ ) than that of PEO ( $0.044 \text{ N m}^{-1}$ ).<sup>23</sup> On the basis of the above TEM and SEM analyses, a schematic presentation of the PS-*b*-PEO/titania hybrid aggregate of HTHs structure is illustrated in Figure 3c.

The internal structure of the PS-*b*-PEO/titania aggregates is highly sensitive to the ambient humidity during the evaporation process.<sup>1,13</sup> As illustrated in Figure 4, the polydisperse PS-*b*-PEO/titania microspheres formed under 67% RH during the evaporation process display a LCVs-like structure. LCVs is another crew-cut morphology of the block copolymer aggregates, bearing some resemblance to that of aggregated soap bubbles. It is supposed to be assemblies of fused vesicles, consisting of many small compartments separated by a copolymer matrix. Both the outer surface of the aggregates and the inner surface of each compartment are covered by short solvophilic chains of block copolymers. In the present study, the PS-*b*-PEO/titania hybrid

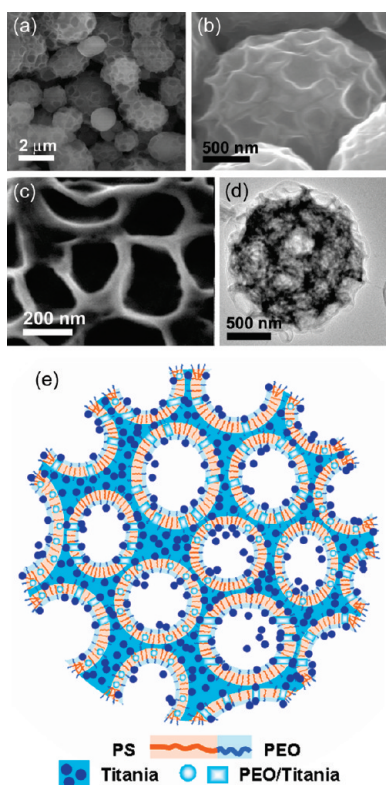


**Figure 4.** (a–c) SEM and (d) TEM images of PS-*b*-PEO/titania hybrid microspheres formed under 67% RH during the evaporation process. (e) Schematic presentation of a PS-*b*-PEO/titania hybrid microsphere of an internal modified LCVs structure.

microspheres exhibit a modified LCVs structure, which shows several differences from the conventional LCVs structures of block copolymer aggregates. First, inorganic species are incorporated into the LCVs structure by binding Ti-oxo species to the hydrophilic PEO chains localized at both the interior and exterior surfaces of the vesicles. Second, bowl-shaped vesicles, instead of spherical vesicles, are dispersed at the aggregate surface. Moreover, a careful examination reveals that the constituent vesicles have holes in the walls, indicating a nonclassical nature of the vesicles (see Figures 4c and 4d);<sup>21</sup> in the present study, the holes may be filled or partially filled with Ti-oxo species. Since the nonclassical vesicles are thought to be an intermediate morphology between classical vesicles and HTHs,<sup>21</sup> our modified LCVs structure could also be regarded as an intermediate morphology between LCVs and HTHs. Both the aggregates and the constituent bowl-shaped vesicles are highly polydisperse, with dimensions in the ranges of 0.5–3  $\mu\text{m}$  and 200–500 nm, respectively, as measured directly from the micrographs. The wall thickness of the constituent vesicles remains relatively uniform ( $\sim 30$  nm), regardless of the vesicle size. A schematic presentation of the PS-*b*-PEO/titania hybrid aggregate with an internal modified LCVs structure is illustrated in Figure 4e.

Thermal decomposition at 500  $^{\circ}\text{C}$  was conducted to remove the block copolymers and obtain inorganic superstructures. As evidenced by the TEM and SEM images (see Figures 5 and 6), the thermal treatment did not disturb the macroscopic shape and the internal morphology of the aggregates significantly, although partial degradation of the internal structure was unavoidable. The titania aggregates prepared under 30% RH appear to be similar to

clews composed of bundles of nanowires after removing the polymer support (see Figures 5a–d). Each nanowire is indeed a chain of nanoparticles and  $\sim 20$  nm in width (Figure 5e), consistent with the width of the PEO/titania domains measured before calcination. The high-resolution TEM images in Figures 5f and 5g show that the nanoparticles are single crystals each, but the junction areas consist of small and randomly oriented crystalline grains. The entire chain and, furthermore, the entire aggregate are polycrystalline in nature. The well-established selected-area diffraction (SAD) pattern reveals that the titania particles are crystallized with anatase phase (Figure 5h). For the titania aggregates prepared under 67% RH, thermal calcination induced partial collapse of the vesicles and the holes inside the walls (see Figures 6a–c). The crystalline phase is also of anatase, as evidenced by the SAD pattern (Figure 6d). Because of the mechanical and physical robustness of the crystalline networks, the aggregates are stable and shape-persistent.

The XRD patterns (Figure 7a) for the titania aggregates calcined at 500  $^{\circ}\text{C}$  exhibit well-established diffraction peaks, which can be ascribed to the (101), (004), (200), (105), (211), and (204) planes of anatase phase. The full width at half-maximum (fwhm) of the (101) peak was further obtained by fitting to a Lorentzian distribution (Figure 7b and 7c), where the calculation of the peak width using the Scherrer equation yielded an average crystallite size of 14.2 and 18.5 nm for the titania aggregates formed under 30% RH and 67% RH during the evaporation process, respectively.

As supporting evidence, the Raman spectra (Figure 7d) of the titania aggregates calcined at 500  $^{\circ}\text{C}$  showed well-established bands at 400, 524, and 640  $\text{cm}^{-1}$ , which are characteristic of the anatase phase, confirming the occurrence of anatase nanocrystallites.

Spectrum A in Figure 8 shows the FTIR transmittance spectrum of PS-*b*-PEO block copolymer. The four bands centered at 700, 760, 1490, and 1600  $\text{cm}^{-1}$ , characteristic of the benzene ring, and the broad band centered at 1115  $\text{cm}^{-1}$ , assigned to the stretching vibration of C–O–C ( $\nu_{\text{C-O-C}}$ ), are due to the presence of PS and PEO blocks, respectively. The bands at 3000–2800  $\text{cm}^{-1}$  and 1485–1330  $\text{cm}^{-1}$  regions are assigned to the stretching vibration ( $\nu_{\text{CH}}$ ) and bending vibration ( $\delta_{\text{CH}}$ ) of  $\text{CH}_2$  groups, respectively. Spectra B and C in Figure 8 are the FTIR spectra of the PS-*b*-PEO/titania hybrid aggregates formed under 30% and 67% RH during the evaporation process, respectively. They evidently confirm the presence of PS-*b*-PEO block copolymers in the hybrids. Besides the bands arising from PS-*b*-PEO, two large bands centered at 3350 and 1640  $\text{cm}^{-1}$ , assigned to the stretching vibration of O–H ( $\nu_{\text{OH}}$ ) and the bending vibration of H–O–H ( $\delta_{\text{OH}}$ ), respectively, are observed for the PS-*b*-PEO/titania hybrids. It reveals that a large number of structure or surface hydroxyl groups and hydroxyl groups from physisorbed water exist in the hybrids. Another broad low-frequency band in the range of 400–1000  $\text{cm}^{-1}$  is observed for the hybrids, which corresponds to the  $\nu_{\text{TiO}_2}$  of the inorganic framework. Its low intensity suggests a low degree of condensation of the inorganic framework. The FTIR analyses indeed confirm the organic/inorganic hybrid nature of the aggregates. Upon calcination at 500  $^{\circ}\text{C}$ , as shown in spectra D and E in Figure 8, the intensity of the Ti–O–Ti vibration band increases, demonstrating an enhanced condensation as the thermal treatment proceeds. In addition, the bands characteristic of hydroxyl groups fade upon thermal treatment, but are still prominent even after calcination at 500  $^{\circ}\text{C}$ . It is reasonable to consider that the contribution from physisorbed water in the porous media and the



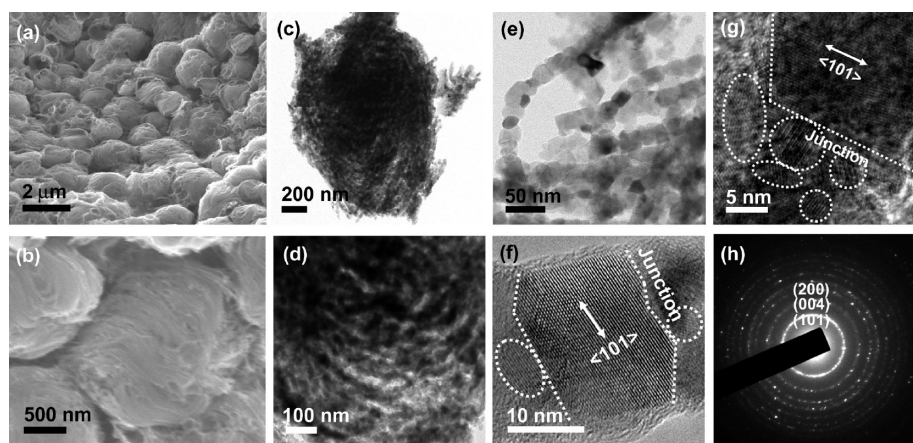


**Figure 5.** (a, b) SEM and (c, g) TEM images of titania aggregates upon calcination at 500 °C. The RH of the evaporation process was controlled at 30%. (h) The SAD pattern of the region shown in panel c.

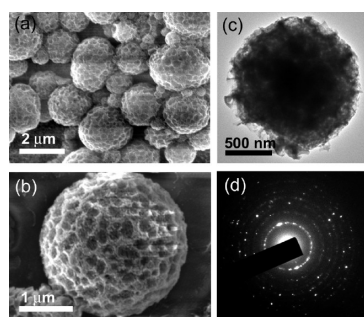


**Figure 6.** (a, b) SEM and (c) TEM images of titania aggregates upon calcination at 500 °C. The RH of the evaporation process was controlled at 67%. (d) The SAD pattern of the region shown in panel c.

structure hydroxyl groups should be insignificant, because the inorganic framework has experienced a high degree of condensation after a relatively severe thermal treatment at 500 °C. Therefore, the appearance of O–H vibration bands at 500 °C indicates the presence of a certain amount of surface hydroxyl groups, probably in the Ti–OH form. It is also indicative of the formation of hydrogen bonds between hydroxyl groups of Ti–OH. The bands corresponding to the block copolymers disappear at 500 °C, indicating an almost complete removal of the copolymer templates and the formation of inorganic aggregates. This is supported by XPS analysis (see Figure S1 in the Supporting Information), where negligible carbon residues were detected in the sample calcined at 500 °C.

**Formation of PS-*b*-PEO/Titania Hybrid Microspheres of Modified LCVs Structure.** Formation of the above unique hybrid crew-cut structures involves the self-assembly of PS-*b*-PEO in selective solvents coupling with the sol–gel chemistry of titania. At the beginning, the block copolymer is completely dissolved in THF, a good solvent for both PS and PEO blocks, at the concentration of 3.8 wt %. Titanium precursors are subsequently added into the system and bind to the hydrophilic PEO blocks through coordination and hydrogen bonds. With the addition of concentrated HCl solution, the system is becoming poor for the PS blocks, such that aggregation of the PS blocks occurs to decrease the interfacial energy between the PS blocks and the surrounding solvents. Although the morphology of the aggregates at this stage is unclear, it is reasonable to speculate that the PS domains are highly

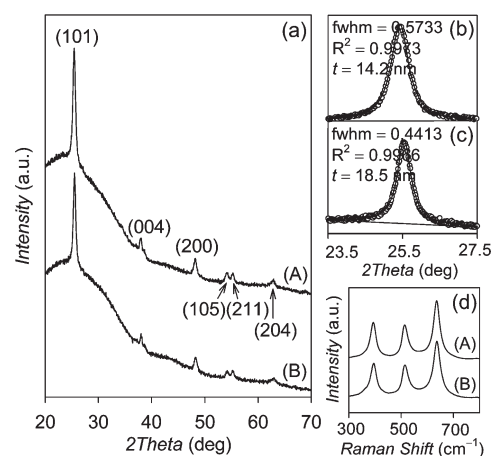


**Figure 7.** (a) XRD spectra of the titania aggregates formed under 30% RH (spectrum A) and 67% RH (spectrum B) during the evaporation process upon calcination at 500 °C. (b) Lineshape of the (101) diffraction peak of the titania aggregates prepared under 30% RH during the evaporation process. (c) Lineshape of the (101) diffraction peak of the titania aggregates prepared under 67% RH during the evaporation process. (d) Raman spectra of the titania aggregates formed under 30% RH (spectrum A) and 67% RH (spectrum B) during the evaporation process upon calcination at 500 °C. The full curves are fit to a Lorentzian distribution.

swollen by THF, because the solubility parameter of THF ( $\delta = 18.6 \text{ MPa}^{1/2}$ ) is very close to that of PS homopolymer ( $\delta = 16.6\text{--}20.2 \text{ MPa}^{1/2}$ ).<sup>24</sup> This leads to a relatively high degree of flexibility of the aggregates. The degree of condensation for the titanium precursors is still low in the acidic solution.

When the solution is drop-cast on a substrate, THF evaporates much faster than water, because THF has a considerably higher vapor pressure than that of water (143 mmHg for pure THF versus 18 mmHg for water at 20 °C). Preferential evaporation of THF concentrates the block copolymer and titanium species in the deposited layer and also increases the relative content of water in the THF/water solvent mixture. As the relative water content increases, the solvent mixture becomes more polar and, thus, poorer for the PS blocks. It leads to a progressive increase in the interfacial energy between the PS blocks and the surrounding solvents. In order to reduce the interfacial energy, PS blocks tend

to aggregate further, in association with an increase in the aggregate size, to decrease the contact area with solvents.<sup>7</sup> The aggregation number also increases with increasing copolymer concentration.<sup>7</sup> As the aggregate size increases, the stretching degree of the PS blocks increases accordingly, which is entropically unfavorable. A morphological change is thus driven to relax the stretching. The dependence of the aggregate size and morphology on the copolymer concentration and the solvent composition has been well-studied for the crew-cut aggregates of block copolymers by Eisenberg and co-workers,<sup>7</sup> who showed that the morphology transitions in the direction from sphere to cylinder and then to bilayer could release the stretching of the core-forming blocks and reduce the entropic penalty. This also applies to the present study.

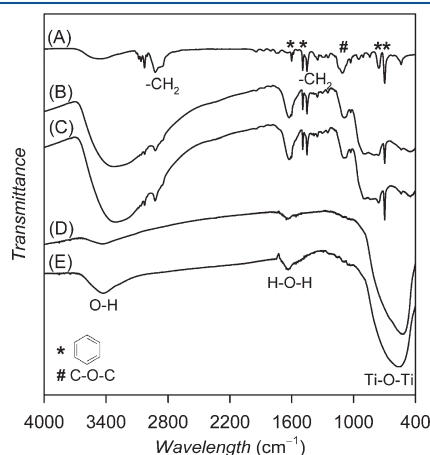


**Figure 8.** FTIR spectra of (A) PS-*b*-PEO (spectrum A), the PS-*b*-PEO/titania hybrid aggregates formed under 30% RH (spectrum B) and 67% RH (spectrum C) during the evaporation process. Also shown are FTIR spectra of the corresponding titania aggregates after calcination at 500 °C (30% RH (spectrum D) and 67% RH (spectrum E)).

We have observed that the structure formed prior to the modified LCVs, as a consequence of the THF preferential evaporation, is apparently a bilayer lamella (see features (A)–(C) in Figure 9a), on the basis of the appearance of intermediate structures trapped during the morphology evolution. This process is slow and capture of intermediate stages is possible, because of the relatively low mobility of the high-molecular-weight block copolymers. According to Zhang and Eisenberg,<sup>25</sup> there are two mechanisms proposed for the formation of LCVs of block copolymers, either by a secondary aggregation of individual vesicles and a subsequent fusion process, or by the bending of one lamella at several places. The formation process, in our case, appears to follow the second mechanism. As illustrated in Figure 9a, first, a lamella bends until it closes to form a relatively large vesicle (see regions (A) and (B)). In general, the curvature at both sides of the lamella differs, because of an uneven distribution of polymer chains of different lengths and, thus, different degrees of corona repulsion.<sup>25</sup> As the polarity of the solvent system increases in association with the preferential evaporation of THF, the difference in the corona repulsions increases; as it reaches a sufficient value, the lamella structure folds spontaneously to form a more favorable vesicular structure.<sup>26</sup> At the same time, the surface of the lamella or vesicle (i.e., closed lamella) caves in at several positions to form relatively small bowl-shaped cavities (region (C)). If there was no TTIP, the sinking movement at the lamella or vesicle surface, which could be stimulated by liquid fluctuation, osmosis pressure, or imbalanced solvent evaporation, would recover due to the repulsion between the PEO chains. However, the presence of TTIP helps to “freeze” the cavity structure. The titanium precursors are affinitive to PEO by forming hydrogen bonds with the hydrophilic PEO chains localizing at the surface of cavities. The titanium species undergo continuous hydrolysis and condensation reactions that bridge adjacent cavities and solidify the structure. Continued cave-in movements eventually give rise to a three-dimensional modified LCVs hybrid structure. The

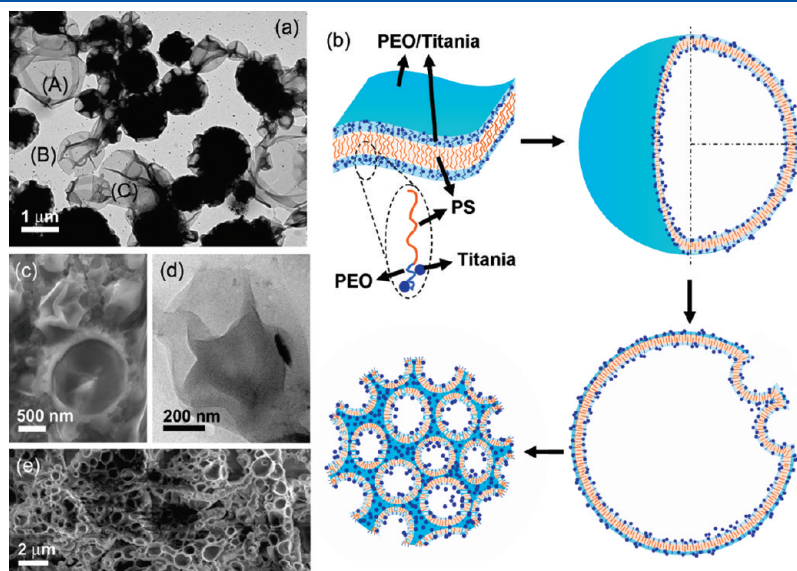


**Figure 9.** (a) TEM image of several trapped intermediate structures (features labeled (A)–(C)) before the formation of the modified LCVs structure. (b) Schematic presentation of the formation mechanism of PS-*b*-PEO/titania hybrid aggregates of an internal modified LCVs structure. (c) SEM and (d) TEM images of the PS-*b*-PEO aggregates prepared by the comparison test. (e) SEM image of the PS-*b*-PEO/titania hybrid aggregates formed without solvothermal treatment.

formation process of the modified LCVs hybrid structure is schematically presented in Figure 9b.

It is obvious that, in the present study, the condensation of titania oligomers is the driving force for the formation of the modified LCVs structure. As supporting evidence, a comparison test was carried out where a solution was prepared following the same procedure to prepare the LCVs hybrids, except that no TTIP was added. Under this condition, only polydisperse individual vesicles of block copolymers were observed (see Figures 9c and 9d). It is deduced that the LCVs structure can be produced either by decreasing the corona repulsion as what happened for block copolymers,<sup>20,27</sup> or by increasing the corona bridging ability as the strategy employed in this study for the preparation of LCVs hybrids.

In addition, the role of HCl in the sol–gel process of titanium species and the formation of the modified LCVs aggregates must be clarified. In the initially deposited sample, HCl acts not only as a catalyst for the hydrolysis of TTIP but also a retardant for the condensation of TTIP. It prevents an otherwise rapid and violent condensation that often results in a precipitation of Ti-oxo species beyond the templating boundary of block copolymers. Along the evaporation process, the continuous exchange of water between the deposited layer and the atmosphere favors a progressive departure of HCl, and it allows gradual condensation of the Ti-oxo species, which is important for the controlled formation and stabilization of the LCVs structure.

Toward the final stage of the evaporation process, as THF is almost completely evacuated the micelle cores, the mobility of polymer chains in the aggregates decreases considerably. The crosslinking of the inorganic species also helps to freeze the aggregate structure. The resultant PS-*b*-PEO/titania hybrids are shape-persistent in the dry status.

The role of the solvothermal treatment appears to affect the macroscopic morphology of the aggregates. As shown in Figure 9e, the aggregates formed without solvothermal treatment are bulky and irregular in shape, but become more or less spherical and smaller in size after experiencing the solvothermal treatment (see Figure 4). This could be well due to the pressure-driven compression effect of the solvothermal process, which is important for orienting the formation of dense structures.

The LCVs structure prepared in this study is different from a typical spongelike structure, although they both possess an irregular porous appearance.<sup>28</sup> The difference lies in the micellar structures from which they are derived. The LCVs structure is templated by vesicular micelles (i.e., spherical “hollow” micelles). The pores are present in the structure before the removal of block copolymers. In contrast, the spongelike structure is templated by spherical “solid” micelles.<sup>28</sup> The pores in titania sponges are generated by removal of the spherical micelles, before which the titania/polymer hybrids are nonporous materials.

**Formation of PS-*b*-PEO/Titania Hybrid Microspheres of HTH Structure.** There are two mechanisms that have been proposed for the formation of crew-cut HTHs of block copolymer aggregates. According to the first mechanism that happens to the PS-*b*-PAA/*N,N*-dimethylformamide/water system,<sup>20</sup> the original aggregates are small and uniform bilayer vesicles; they fuse to form LCVs and subsequently rearrange to a HTHs pattern. The structure transition is driven by a reduction in the effective volume fraction of the corona-forming PAA blocks caused by ion addition. It resembles the phase behavior of block copolymers in bulk that changes from bilayer lamellae to hexagonally packed cylinders. However, the hollow rods in the HTHs form hoops to avoid the

end-capping energy penalty, which is larger than the curvature energy in the size range studied.

According to the second mechanism, which involves the PS-*b*-PEO/THF/water system,<sup>21</sup> the original aggregates are large and polydisperse bilayer vesicles. The transition proceeds in three steps: (1) formation of hollow regions in the vesicle walls (nonclassical vesicles), accompanied by a thickening of the walls and gradual disappearance of the vesicle cores; (2) alignment of some rods to form quasi-hexagonal structures; and (3) development of the HTHs structure. The degree of the PS chain stretching remains almost constant during the morphological transition from classical to nonclassical vesicles. It indicates a lesser contribution of the core stretching to the structural evolution. The morphology transition is largely determined by the variation of the corona repulsive strength.

The above two mechanisms involve very different starting stages, depending on whether a vesicle fusion process is involved, but have considerable similarity in the latter stages of the morphology evolution. The early stage difference also arises from a difference in the corona repulsive strength for the precursor vesicles.<sup>21</sup>

In the present study, when the environment of the evaporation process was changed from 67% RH to 30% RH, a HTHs hybrid structure was resulted. RH is defined as the percentage of the actual vapor pressure, relative to the saturated vapor pressure of water in air at a prescribed temperature. A lower RH means a smaller partial vapor pressure of water in air, which will drive faster water evaporation. Consequently, the solvent in the deposited layer, which is dried under a lower humidity, will become less polar, because it is composed of a smaller water content; water has a much higher dielectric constant ( $\epsilon_{\text{H}_2\text{O}} = 80.1$ ) than THF ( $\epsilon_{\text{THF}} = 7.5$ ) which indicates the polarity of solvent.<sup>24</sup> It is known that a lower polarity of the solvent leads to a weaker PEO–solvent interaction, which decreases both the PEO coil dimension and the repulsive interactions among the PEO corona chains.

Therefore, the phase transition with the humidity variation bears some resemblance to the phase behavior of block copolymers in bulk. For the modified LCVs aggregates formed under 67% RH, the constituent bilayer vesicles could be regarded as having approximately equal effective volume fractions of the PS blocks and the PEO/Ti-oxo species. Compared to this, the aggregates formed under a lower humidity environment (e.g., RH = 30%), which is associated with a reduced dimension and, thus, reduced effective volume fraction of the PEO blocks, undergo a morphology transition from bilayer vesicles to hexagonal structures. This is in parallel with the phase behavior in bulk from lamellae to hexagonally packed cylinders as the effective volume fraction of one component decreases.

Indeed, as mentioned earlier, our modified LCVs structure is composed of nonclassical vesicles, which have pores in the walls. It is regarded as an intermediate structure between LCVs and HTHs. Also, certain bowl-shaped vesicles were found at the surface of the HTHs hybrids, as evidenced by both TEM (Figure 1e and 2c') and SEM (Figure 3a) images. These observations suggest that there is a relationship between the modified LCVs and HTHs structures, and there can be a phase transition between them.

## CONCLUSIONS

PS-*b*-PEO/titania hybrid microspheres of an internal hexagonally packed titania hoops (HTHs) or modified large compound vesicles (LCVs) morphology were developed by coupling



the self-assembly of PS-*b*-PEO in selective solvents with the sol–gel chemistry of titania. HTHs refers to the structure composed of titania hoops hexagonally packed in the PS matrix; both the external aggregate surface and the interface between the titania hoops and the PS matrix are lined with PEO chains. This is the first time that the HTHs structure has been reported; it involves the mineralization of HTHs and constitutes an additional morphology seen in the crew-cut hybrids. The modified LCVs aggregates are essentially polydisperse spheres, containing nonclassical vesicles linked by Ti-oxo networks; bowl-shaped vesicles are dispersed at the aggregate surface. The morphological formation and evolution observed in the present study is obviously complicated by the multiplicity of factors involved, i.e., the humidity of the evaporation process, the evaporation rate of solvents, the water/tetrahydrofuran (water/THF) contents, the polymer concentration, and the sol–gel chemistry of titania. All of these factors influence the observed morphology. Formation of the modified LCVs structure first involves the occurrence of a lamella structure. On continued preferable THF evaporation and water accumulation, the system experiences several steps: folding of the lamellae to form large polydisperse vesicles, caving in at the vesicle surface to form bowl-shaped vesicles, cross-linking of the titanium precursors to solidify the cavity structure, and continued cave-in movements to form a three-dimensional LCVs structure. Formation of the HTHs structure involves a morphological transition from the modified LCVs as the relative humidity of the evaporation process decreases from 67% to 30%. This is ascribed to the reduction in the effective volume fraction of the PEO blocks associated with the decrease in humidity. The hybrids of an internal HTHs or modified LCVs morphology were converted to the corresponding porous titania aggregates upon calcination at 500 °C, where the amorphous titania phase changed to the anatase crystalline phase. The present study clearly reveals that the inorganic or hybrid nanostructures templated by crew-cut assemblies can significantly expand the range of accessible morphologies, which provides the potential for novel and advanced applications in drug delivery, coatings, solar energy conversion, and photocatalysis.

## ■ ASSOCIATED CONTENT

**S Supporting Information.** XPS spectra of the PS-*b*-PEO/titania hybrid microspheres and the corresponding titania aggregates calcinated at 500 °C. This information is available free of charge via the Internet at <http://pubs.acs.org/>.

## ■ AUTHOR INFORMATION

### Corresponding Author

\*Phone: +65 65161268. Fax: +65 67763604. E-mail: msewangj@nus.edu.sg.

## ■ ACKNOWLEDGMENT

This work is supported by the National University of Singapore (Tier 1 grant, R284-000-054-112) and the Science and Engineering Research Council - A\*Star, Singapore (Grant No. 072 101 0013).

## ■ REFERENCES

- (1) Cheng, Y.-J.; Gutmann, J. S. *J. Am. Chem. Soc.* **2006**, *128*, 4658.
- (2) (a) Soler-Illia, G. J. de A. A.; Sanchez, C.; Lebeau, B.; Patarin, J. *Chem. Rev.* **2002**, *102*, 4093. (b) Soler-Illia, G. J. de A. A.; Crepaldi, E. L.;

- Grosso, D.; Sanchez, C. *Curr. Opin. Colloid Interface Sci.* **2003**, *8*, 109. (c) Crepaldi, E. L.; Soler-Illia, G. J. de A. A.; Grosso, D.; Cagnol, F.; Ribot, F.; Sanchez, C. *J. Am. Chem. Soc.* **2003**, *125*, 9770. (d) Smarsly, B.; Grosso, D.; Brezesinski, T.; Pinna, N.; Boissière, C.; Antonietti, M.; Sanchez, C. *Chem. Mater.* **2004**, *16*, 2948. (e) Fisher, A.; Kuemmel, M.; Jarn, M.; Linden, M.; Boissière, C.; Nicole, L.; Sanchez, C.; Grosso, D. *Small* **2006**, *2*, 569.
- (3) (a) Brezesinski, T.; Groenewolt, M.; Gibaud, A.; Pinna, N.; Antonietti, M.; Smarsly, B. M. *Adv. Mater.* **2006**, *18*, 2260. (b) Fattakhova-Rohlfing, D.; Wark, M.; Brezesinski, T.; Smarsly, B. M.; Rathouský, J. *Adv. Funct. Mater.* **2007**, *17*, 123. (c) Brezesinski, T.; Antonietti, M.; Smarsly, B. M. *Adv. Mater.* **2007**, *19*, 1074.
- (4) (a) Choi, S. Y.; Mamak, M.; Coombs, N.; Chopra, N.; Ozin, G. A. *Adv. Funct. Mater.* **2004**, *14*, 335. (b) Choi, S. Y.; Lee, B.; Carew, D. B.; Mamak, M.; Peiris, F. C.; Speakman, S.; Chopra, N.; Ozin, G. A. *Adv. Funct. Mater.* **2006**, *16*, 1731.
- (5) Smart, T.; Lomas, H.; Massignani, M.; Flores-Merino, M. V.; Perez, L. R.; Battaglia, G. *Nanotoday* **2008**, *3*, 38.
- (6) Zhang, L.-F.; Eisenberg, A. *Science* **1995**, *268*, 1728.
- (7) Choucair, A.; Eisenberg, A. *Eur. Phys. J. E* **2003**, *10*, 37.
- (8) Wang, M.-F.; Zhang, M.; Siegers, C.; Scholes, G. D.; Winnik, M. A. *Langmuir* **2009**, *25*, 13703.
- (9) Zhu, J.-T.; Hayward, R. C. *J. Am. Chem. Soc.* **2008**, *130*, 7496.
- (10) Cheng, Y.-J.; Zhi, L.-J.; Steffen, W.; Gutmann, J. S. *Chem. Mater.* **2008**, *20*, 6580.
- (11) Cheng, Y.-J.; Müller-Buschbaum, P.; Gutmann, J. S. *Small* **2007**, *3*, 1379.
- (12) Cheng, Y.-J.; Zhou, S.-Y.; Gutmann, J. S. *Macromol. Rapid Commun.* **2007**, *28*, 1392.
- (13) Perlich, J.; Schulz, L.; Kashem, M. M. A.; Cheng, Y.-J.; Memesa, M.; Gutmann, J. S.; Roth, S. V.; Müller-Buschbaum, P. *Langmuir* **2007**, *23*, 10299.
- (14) Peng, J.; Li, X.; Kim, D. H.; Knoll, W. *Macromol. Rapid Commun.* **2007**, *28*, 2055.
- (15) Li, X.; Peng, J.; Kang, J.-H.; Choy, J. H.; Steinhart, M.; Knoll, W.; Kim, D. H. *Soft Matter* **2008**, *4*, 515.
- (16) Li, X.; Yang, H.; Li, C.-S.; Xu, L.-M.; Zhang, Z.-G.; Kim, D. H. *Polymer* **2008**, *49*, 1376.
- (17) Du, J.-Z.; Chen, Y.-M.; Zhang, Y.-H.; Han, C.-C.; Fisher, K.; Schmidt, M. J. *J. Am. Chem. Soc.* **2003**, *125*, 14710.
- (18) Du, J.-Z.; Chen, Y.-M. *Angew. Chem., Int. Ed.* **2004**, *43*, 5084.
- (19) Yu, K.; Hurd, A. J.; Eisenberg, A.; Brinker, C. J. *Langmuir* **2001**, *17*, 7961.
- (20) Zhang, L.-F.; Bartels, C.; Yu, Y.-S.; Shen, H.-W.; Eisenberg, A. *Phys. Rev. Lett.* **1997**, *79*, 5034.
- (21) Yu, K.; Bartel, C.; Eisenberg, A. *Langmuir* **1999**, *15*, 7157.
- (22) Yu, K.; Bartels, C.; Eisenberg, A. *Macromolecules* **1998**, *31*, 9399.
- (23) Thomas, H. R.; O'Malley, J. J. *Macromolecules* **1979**, *12*, 323.
- (24) Yu, Y.-S.; Zhang, L.-F.; Eisenberg, A. *Macromolecules* **1998**, *31*, 1144.
- (25) Yu, K.; Eisenberg, A. *Macromolecules* **1998**, *31*, 3509.
- (26) Shen, H.-W.; Eisenberg, A. *J. Phys. Chem. B* **1999**, *103*, 9473.
- (27) Zhang, L.-F.; Yu, K.; Eisenberg, A. *Science* **1996**, *272*, 1777.
- (28) Perlich, J.; Kaune, G.; Memesa, M.; Gutmann, J. S.; Müller-Buschbaum, P. *Philos. Trans. R. Soc. A* **2009**, *367*, 1783.